MICHIGAN STATE UNIVERSITY

CYCLOTRON LABORATORY

NEUTRON EMISSION FROM COLLISIONS OF ^{14}N NUCLEI AT 35 MeV/u*

B. A. Remington, G. Caskey, A. Galonsky, C.K. Gelbke, M.B. Tsang, Z. Seres, F. Deak, A. Kiss, J. Kasagi and J.J. Kolata

Invited talk at the

4th INTERNATIONAL CONFERENCE
ON NUCLEAR REACTION MECHANISMS

Villa Monastero, Varenna, 10-15 June 1985

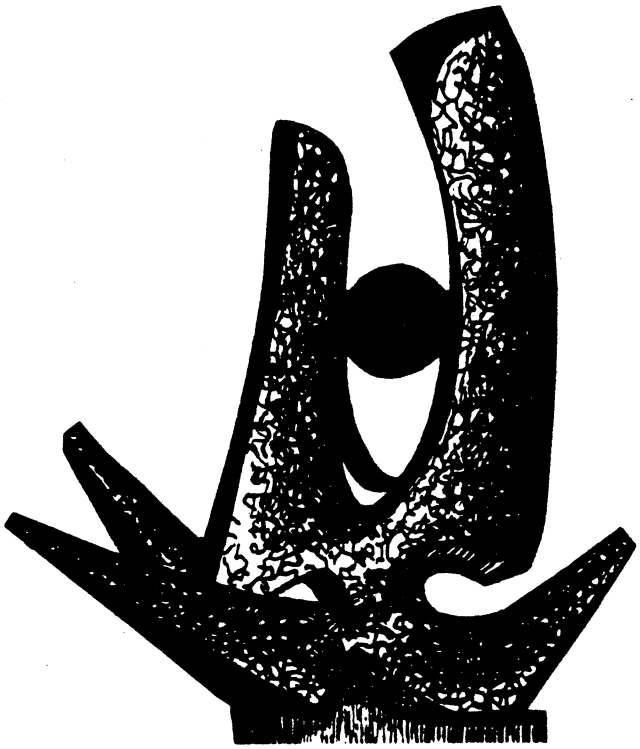

JULY 1985

MSUCL-531

NEUTRON EMISSION FROM COLLISIONS OF ^{14}N NUCLEI AT 35 MeV/u[#]

B.A. Remington, G. Caskey, A. Galonsky*, C.K. Gelbke, and M.B. Tsang
Physics Department and Cyclotron Laboratory
Michigan State University
E. Lansing, MI 48824, USA,

Z. Seres
Central Research Institute, POB 49, H-1525 Budapest Hungary,

F. Deak and A. Kiss
Eotvos University, Puskin ut 5-7, H-1088 Budapest, Hungary,

J. Kasagi
Tokyo Institute of Technology, Meguro-ku, Tokyo, Japan, and

J.J. Kolata
University of Notre Dame, Notre Dame, IN 46556, USA

1. Introduction - When nuclei collide with a kinetic energy of several hundred MeV, a large part of that kinetic energy may be converted into short-lived excitation energy. The favorite way of fast de-excitation is the emission of nucleons and of light nuclei up to the alpha particle. Among these particles only the neutrons follow paths that are free of Coulomb distortions as they leave the region of interaction. At least in principle, then, the neutrons should carry a clean message of the early part of the reaction, and the use of their special property in fragment-neutron coincidence experiments [1-3] has taught us a great deal about reaction mechanisms.

   Our experiment was not very different from the others; the geometrical arrangement can be seen in Fig. 1. The analysis was also not very different; neutron spectra in coincidence with projectile fragments (PF) were fitted with moving sources. But some of the source parameters turned out to be quite different.

2. Some experimental details - The targets (Ho, Ni, and C) were bombarded by a beam of ^{14}N nuclei at 490 MeV that is, 35 MeV/u. The targets and several ΔE - E Si telescopes for PF detection were inside a thin-walled

[#]Supported by NSF grants PHY 83-12245 and INT 80-15333
*Presented paper.

chamber, and ten neutron scintillation detectors were outside the chamber at distances of ~1.5-2.5 m from the center. One of the set ups used is sketched in Fig. 1. Each neutron detector had a thin, charged - particle anticoincidence scintillator in front of it. The shadow bars shown in the figure were in place part of the time for measurement of background - mostly neutrons scattered into the detectors by the floor. Ten percent is a typical value for the background. The detection efficiency is energy dependent, and again 10% is a typical value for this quantity.

When a neutron was in coincidence with a fragment, the neutron energy was determined from the time difference between the two particles plus the time of flight of the fragment. The latter time could easily be computed from the telescope signals; they fixed the element and isotope and also the energy of the fragment.

3. Results - Fragments were detected at six angles between 7° and 30°. For a target of Ho (only the Ho data will be discussed in this report) the energy spectra of carbon fragments is given in Fig. 2, at 10° in the bottom part of the figure and at 23° at the top. At 10° two regions are identified - quasielastic (QE) and strongly damped (SD). At 23° perhaps a remnant of the QE survives. At 30° (not shown) there is not even a remnant, and at 7° (also not shown) the SD part is hard to discern. The spectra of other PFs - Li, Be, and B- have the same features as the C spectra. In the extreme there are clearly two kinds of collisions, glancing and head-on, and by choice of angle either one can be emphasized over the other.

We can expect to see different features in the neutron spectra associated with these two kinds of collisions. With a glancing collision we might see neutrons from a surface hot spot. Attenuation by the big Ho nucleus would then create a left-right asymmetry. Since the grazing angle is 8°, we would expect a QE fragment at 10° to have undergone positive-angle scattering. Hence, the asymmetry associated with QE scattering to the right would be a diminished neutron intensity on the left. We have reported [4] a left-right asymmetry, but it is of the opposite sign! The effect is illustrated in Fig. 3, a velocity scatter plot for neutrons at each of the ten angles shown in Fig. 1. The neutrons are in coincidence with QE boron fragments at 10° on the right. Instead of a hot spot sitting on the surface of the target nucleus, we must imagine the neutron source to result from the transfer of nucleons from the ^{14}N projectile to a part of the target. The leftward momentum

of this source balances the rightward momentum of the QE fragment at 10°. The velocity of the source produces the left-side enhancement. The greater the mass of the QE fragment at 10°, the lighter the source, the greater its velocity must be, and the greater the asymmetry. This is in accord with observation[4] - perhaps no asymmetry for PF=Li, but ever-increasing asymmetry for PF = Be,B,C. Qualitatively this agrees with the model[5] of promptly emitted particles.

Other aspects of the data may be seen in the neutron multiplicity spectra of Fig. 4. These spectra give the number of neutrons per sr and per MeV per QE boron fragment emitted at 10°. All ten spectra are presented. The spectra that extend to ~100MeV are for ±10°; those that terminate ~20 MeV are for ±160°; and the others are for intermediate angles. We focus on three features of the data. 1) At the lowest energies the multiplicity decreases at about the same rate for all angles; even the absolute values are constant to within a factor-of-two. 2) There are long, high-energy tails at the forward angles; even at 20 MeV the absolute values differ by more than a factor of 100. 3) The spectra at ±10° (the two at the top) are approximately equal below 15MeV and above 40MeV, but between 15 and 40 MeV the +10° spectrum is higher than the -10° spectrum--more than a factor-of-five at 25-30 MeV. Spectra gated by other fragments (Li, Be, or C) at 10°, whether QE or SD, have the same three features. Spectra gated by a PF at other angles have the first two features and, in a neutron detector directly behind a fragment detector, the big bump also. How can we understand all this? A model that has the appeal of possible physical reality is the model of moving-thermal sources. It is obvious, however, that feature 3 is outside of this model. The big bump is produced by neutrons emitted with low energy from the parent PF and then swept along with the PF by its high velocity, i.e., by kinematic focusing[6]. Therefore, the three spectra at angles near the PF direction were temporarily put aside, and the remaining spectra were fitted with two thermal sources. This was done for PF angles of 10° and 30°, for fragments of Li, Be, B, and C, and for each of five fragment energy bins. The results for one case, B at 10° with 14-21 MeV/u, are shown in Fig. 5. The unfitted spectra are those at 30°, 10°, and -10°; they are the only spectra that have neutrons in excess of those produced by the two sources. In Fig. 6 we examine the fits for different B fragment energy gates on the neutrons in a single detector, at -30°, which is 40° from the fragment direction. Everything fits. In Fig. 7 we do the same for neutrons and fragments both at 10°. The curves consistently fit the data at only the very low

energies. So the two-source model fits all except the contribution from excited PFs.

What about the parameters of the sources? Each has four-a strength, a temperature, a direction, and a speed. One source moves very slowly, with E/A~0.1MeV. Therefore, this source may be called target-like. It is responsible for the almost-isotropic low-energy neutrons.Its temperature, which is between 2 and 3 MeV, is independent of the species of the PF; it depends only on the loss of kinetic energy of the projectile. The other source moves very rapidly, with E/A~8MeV, i.e., at about half the projectile velocity. Its temperature is always about 8 MeV. The combination of high velocity and high temperature enable it to produce the forward-peaked, high-energy neutrons. [This fast, hot source is the same as the intermediate-rapidity source used to fit the high-energy portions of charged particle spectra.[7]] With an SD gate on the PF this source moves at 0°, but with a QE gate the source moves to the side opposite the PF and produces the observed neutron asymmetry. The direction of the target-like source is irrelevant because it moves so slowly. The strengths of the sources are presented in Fig. 8. There is a maximum of about ten neutrons per fragment at 10°. In a manner that does not depend on the PF species, the strength (or multiplicity) decreases as the PF energy increases, i.e., as the source excitation energy decreases. And always the strengths of the two sources track together, the fast hot source producing ~ 1/4 as many neutrons as the target-like source.

Finally, we come back to the unfitted spectra, such as the ones for co-linear PF and neutron directions shown in Fig. 7. There one can see the correlation between peak energy and PF energy per nucleon. To account for the neutrons in excess of those predicted by the two thermal sources we had to look at energy levels of boron nuclei. A level at 3.388 MeV in ^{12}B decays to the ground state of ^{11}B with the emission of a 19-keV neutron. This process, along with standard kinematics of velocity addition and solid-angle transformation, provides the bulk of the missing neutrons. The next state in ^{12}B, at 3.76 MeV, provides most of the rest. In Fig. 9 we see the excess for one of the spectra, the circles, and its excellent fit by this mechanism, the histogram. The only parameters are the strengths of the sources; all else is kinematics.

For other species of PF it is necessary to invoke the same mechanism, but of course with different energy levels. We can make transparent the fact that we are dealing with low-energy neutrons by

sorting out PF-neutron events according to velocity difference. For the co-linear 10° geometry we show the results of such sorting for three different PF species in Fig. 10. For B the neutron energy is so low that virtually all neutrons are dragged along with the B fragment. For Li the energy is higher, 0.26 MeV, and we get a forward peak and a backward peak centered on zero velocity difference. For C at least two decays are prominently involved, and we get four peaks. A seperate report is being prepared on the velocity spectra.

4. Conclusions - From the spectra of neutrons in coincidence with projectile fragments we have the picture that those collisions result in three excited fragments - 1) A slowly-moving target-like fragment at a temperature of 2-3 MeV, depending on how peripheral (QE) or central (SD) the collision is. 2) A fast (half beam velocity), hot ($T \gtrsim 8$ MeV) fragment. In peripheral (QE) collisions this excited fragment moves off axis, recoiling against the PF. In central (SD) collisions it moves on axis, perhaps emitting both neutrons and the PF. Restricted by energy conservation the fast, hot fragment has mass number $A \lesssim 25$. 3) A PF in its various excited states. As this is not a thermal source, its contribution to neutron or proton spectra, in inclusive measurements, for example, should not be included when a slope and a temperature are determined.

References

1. D. Hilscher, J.R. Birkelund, A.D. Hoover, W.U. Schröder, W.W. Wilcke, J.R. Huizenga, A.C. Mignerey, K.L. Wolf, H.F. Breuer, and V.E. Viola, Phys. Rev. C20, 576 (1979).

2. Y. Eyal, A. Gavron, I. Tserruya, Z. Fraenkel, Y. Eisen, S. Wald, R. Bass, C.R. Gould, G. Kreyling, R. Renfordt, K. Stelzer, R. Zitzman, A. Gobbi, U. Lynen, H. Stelzer, I. Rode, and R. Bock, Phys. Rev. C21, 1377 (1980).

3. E. Holub, D. Hilscher, G. Ingold, U. Jahnke, H. Orf and H. Rossner, Phys. Rev. C28, 252 (1983).

4. G. Caskey, A. Galonsky, B. Remington, M.B. Tsang, C.K. Gelbke, A. Kiss, F. Deak, Z. Seres, J.J. Kolata, J. Hinnefeld and J. Kasagi, Phys. Rev. C31, 1597 (1985).

5. J.P. Bondorf, J.N. De, G. Fai, A.D.T. Karvinen, B. Jakobsson and J. Randrup, Nucl. Phys. A333, 285 (1980).

6. A. Gavron, J.R. Beene, R.L. Ferguson, F.E. Obenshain, F. Plasil, G.R. Young, G.A. Petitt, K. Geoffroy Young, M. Jaaskelainen, D.G. Sarantites, and C. F. Maguire, Phys. Rev. C 24, 2048 (1981).

7. B.V. Jacak, G.D. Westfall, C.K. Gelbke, L.H. Harwood, W.G. Lynch, D.K. Scott, H. Stocker, M.B. Tsang, and T.J.M. Symons, Phys. Rev. Lett., 51, 1846, (1983).

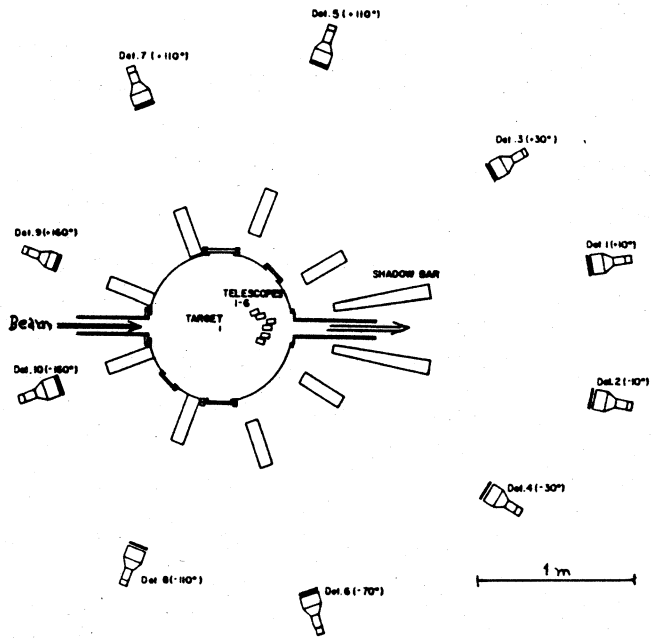

Figure 1. Typical layout of the experiment.

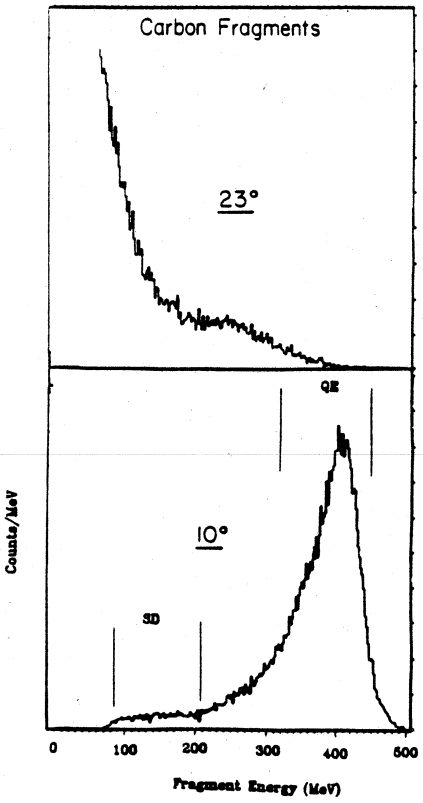

Figure 2. Spectra of carbon fragments at 10° (bottom) and 23° (top).

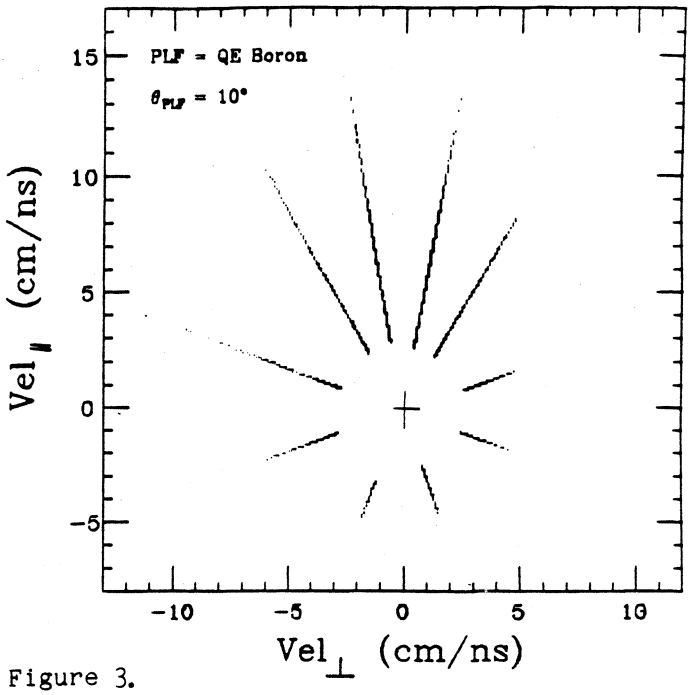

Figure 3.

Velocity scatter plot for neutrons detected at ± 10°, ±30°, ±70°, ±110°, and ±160°. The neutrons are in coincidence with quasi-elastic boron fragments at +10°, that is, at 10° to the right. Note the enhanced neutron intensity on the left.

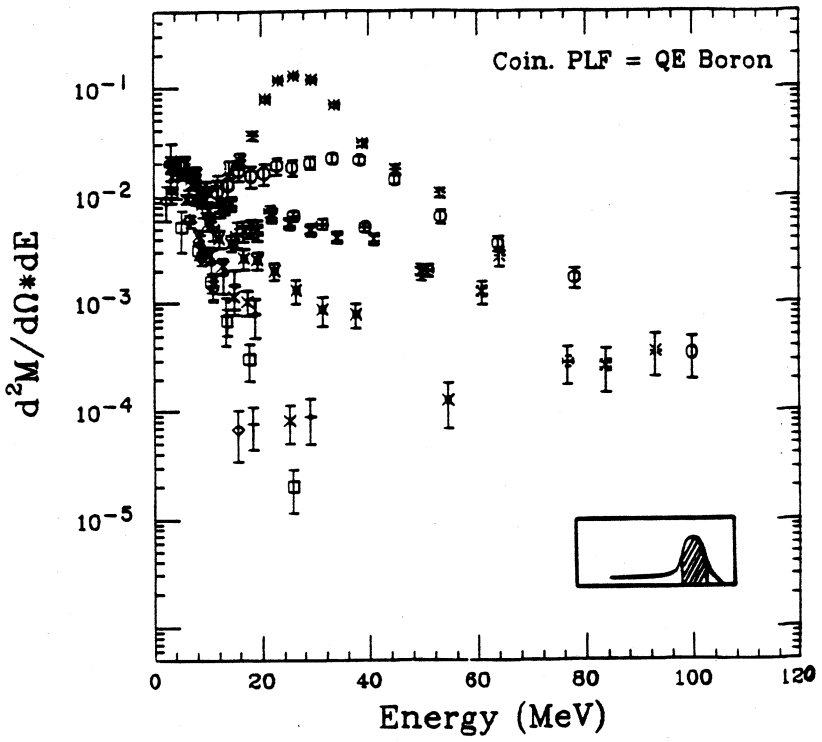

Figure 4.

Neutron energy spectra at angles ranging from 10° to 160°. The neutrons are gated by quasi-elastic boron fragments at 10°. The multiplicity units are neutrons per steradian per MeV per coincident fragment.

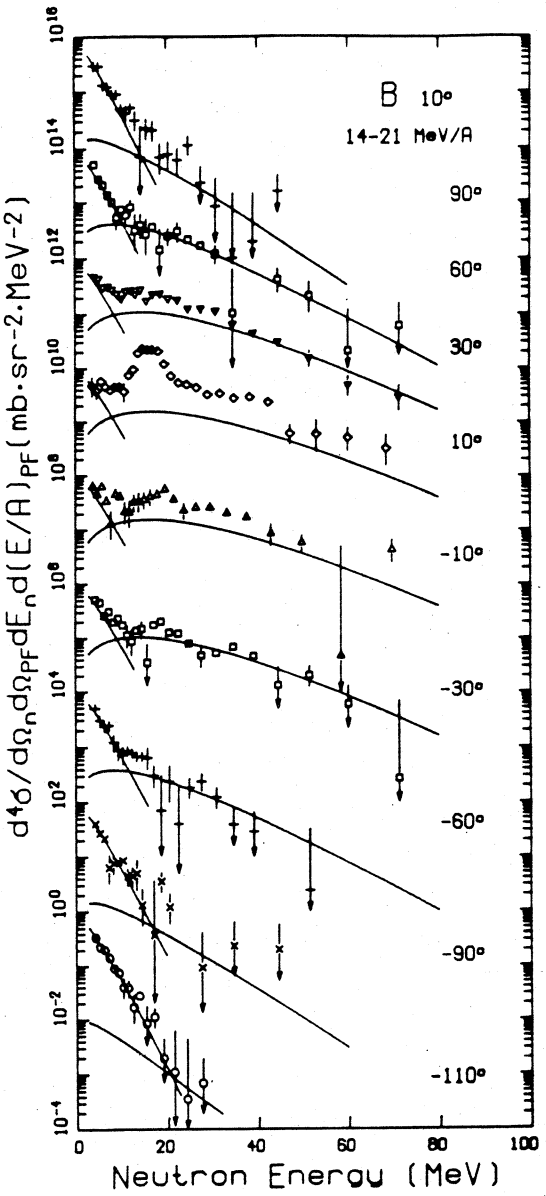

Figure 5

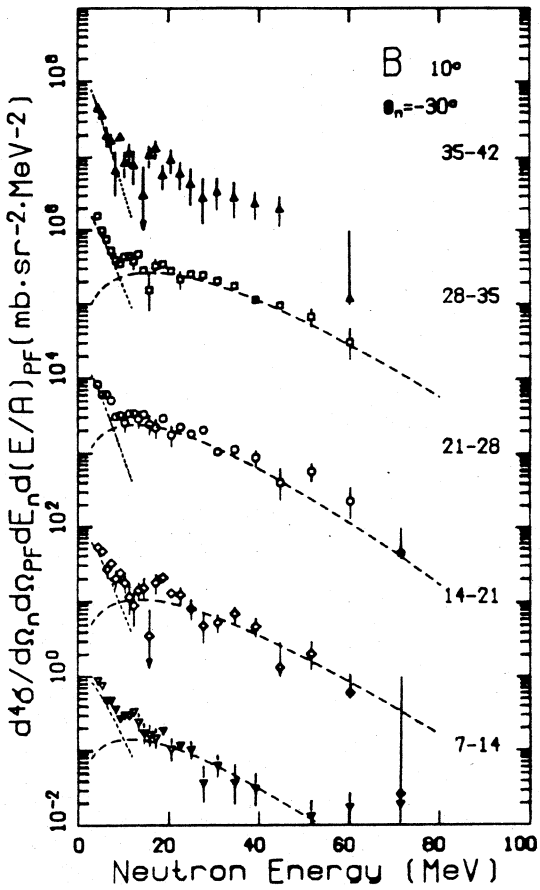

Figure 6

Figure 5.
Neutron energy spectra at the indicated angles between 10° and 110°. The neutrons are gated by boron fragments at 10° having energy-per-nucleon between 14 and 21 MeV. The vertical scale is correct for the spectrum at the bottom. For each subsequent spectrum above it the scale should be multiplied by 10^{-2}. The curves are results of two-source fits to all the data except those at 30°, 10°, and -10°.

Figure 6.
Neutron energy spectra at -30°. The neutrons are gated by boron fragments at 10° in the five indicated intervals of energy-per-nucleon. The vertical scale and the curves are as in Fig. 5.

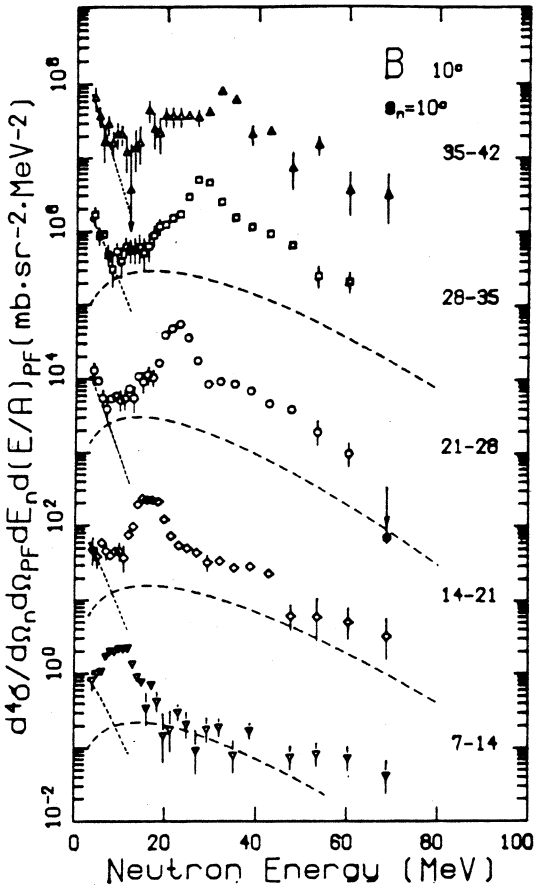

Figure 7

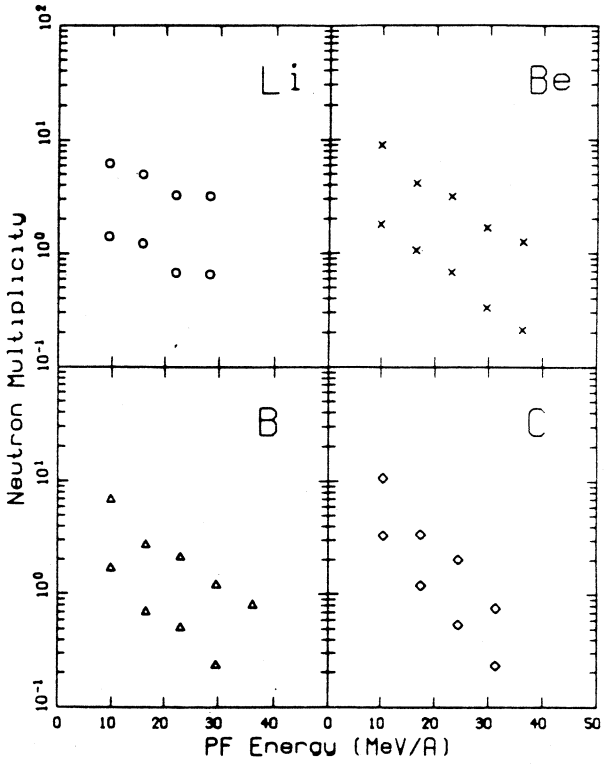

Figure 8

Figure 7. Neutron energy spectra at 10°. Remainder of caption same as Fig. 6.

Figure 8. Neutrons at all angles and energies per fragment-at-10° versus fragment energy for the indicated fragment species. In each quadrant the upper set of points relates to the target-like source and the lower set to the fast, hot source.

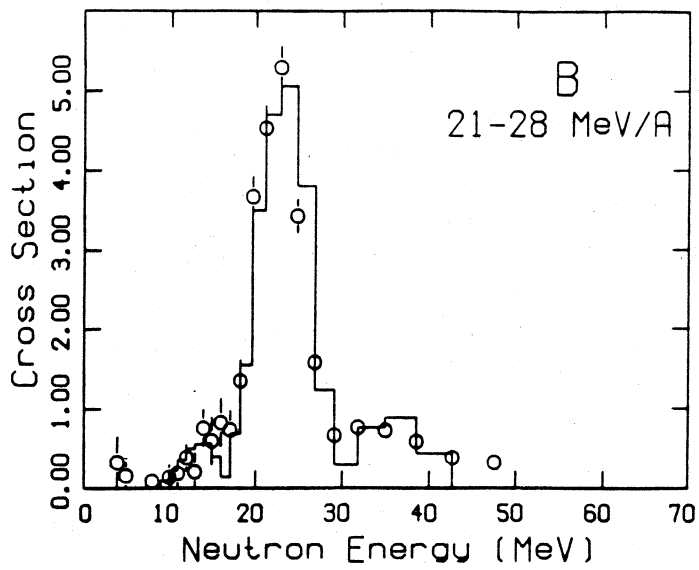

Figure 9.

The middle spectrum of Fig. 7. Only the excess over that produced by the two thermal sources is plotted (the circles). The histogram is a Monte Carlo fit based on neutron emission from moving ^{12}B fragments in the 3.39 - and 3.76 - MeV excited states.

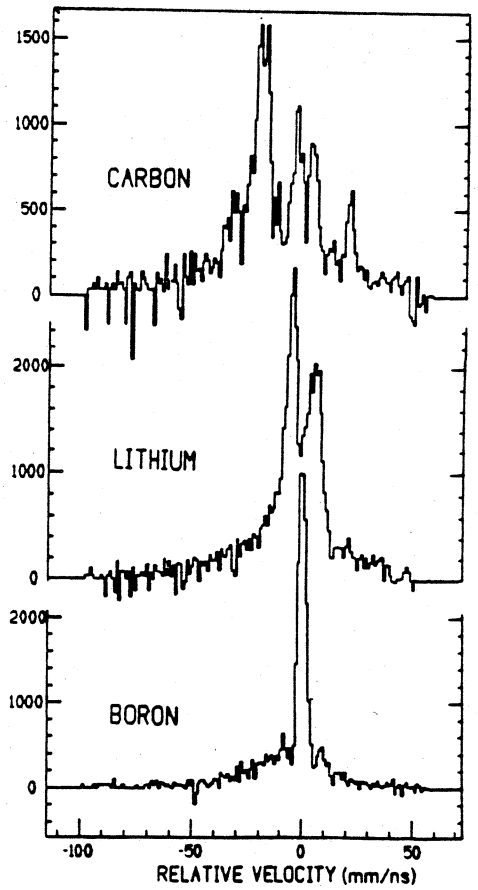

Figure 10.

Spectra of the velocity difference between fragments and neutrons detected at the same angle, 10°. The fragments and neutrons covered energy ranges of more than 100 MeV and 50 MeV, respectively, but the width of the boron peak, for example, is less than 0.2 MeV.